Fusion-fission cross sections for $^{32}S + ^{138}Ba$ and $^{48}Ti + ^{122}Sn$ at near-barrier energies

A. Charlop, J. Bierman, Z. Drebi, S. Gil,* A. Sonzogni, R. Vandenbosch, and D. Ye
University of Washington, Nuclear Physics Laboratory GL-10, Seattle, Washington 98195
(Received 7 March 1994)

The fission cross sections for $^{32}S + ^{138}Ba$ and $^{48}Ti + ^{122}Sn$ in the region of the fusion barrier have been measured. These results are combined with evaporation residue cross sections from another measurement to obtain the total fusion excitation functions for these systems at energies near and below the barrier. Coupled channels calculations easily reproduce the experimental results.

PACS number(s): 25.70.Jj, 24.10.Eq

I. INTRODUCTION

There has been a considerable interest in heavy-ion fusion reactions at energies near and below the barrier in recent years. Much of the work to date has focused on reactions that produce compound nuclei with mass greater than 150 [1]. In these heavy systems, fission can be a significant fraction of the total fusion cross section.

The present work is part of a program to study the spin distribution of the compound nucleus, ^{170}Hf, formed in fusion reactions at sub- and near-barrier energies. The program looks at three systems, $^{28}Si + ^{142}Ce$, $^{32}S + ^{138}Ba$, and $^{48}Ti + ^{122}Sn$. These systems vary the mass asymmetry in the entrance channel. All three systems produce the same compound nucleus in a similar excitation energy range at bombarding energies near and below the Coulomb barrier. The primary goal of the program is to look for possible entrance channel effects in heavy-ion fusion reactions at energies near and below the barrier. This is accomplished through a comparison of the energy dependence of the compound nucleus mean spin of the three systems and with a coupled channels model which fits the fusion excitation functions.

The evaporation residue cross sections were measured previously for all three systems and are discussed elsewhere [2]. These cross sections were determined using a delayed x-ray technique developed by DiGregorio *et al.* [3]. The evaporation residue cross sections were measured from 20% above the barrier to approximately 10% below the barrier for each system. The partial cross section for each evaporation residue is determined from the x-ray activities of the residue and its daughters. The sum of all the partial cross sections gives the evaporation residue cross section. This technique, however, is not sensitive to fission products. The coupled channels code CCDEF [4] used to fit the excitation functions calculates the total fusion cross section. Therefore, the fission cross section needs to be estimated or experimentally measured.

The fission cross section also plays an important part in the determination of the total mean spin of the compound nucleus. The energy dependence of the mean spin of the compound nucleus has been measured for these systems and will be discussed in an upcoming publication [5]. The γ-multiplicity method used in determining the mean spin is insensitive to the fission branch of the fusion cross section. At energies where fission is a significant fraction of the total cross section, the contribution of the fission channel to the mean spin may be large.

II. EXPERIMENTAL SETUP

The beams of ^{32}S and ^{48}Ti were produced using the FN Tandem accelerator and Superconducting Linac at the University of Washington Nuclear Physics Lab. The beam was tuned into a 60-in.-diam. scattering chamber. Fig. 1 shows a schematic of the scattering chamber setup.

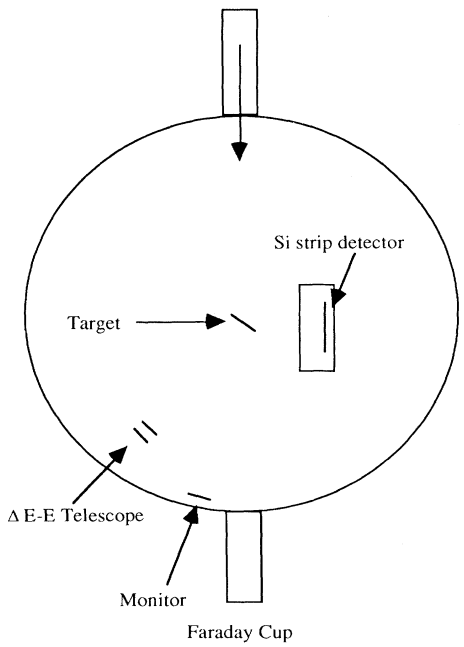

FIG. 1. Experimental setup.

*Present address: Tandar, Departamento de Fisica, CNEA, Buenos Aires, Argentina.

TABLE I. Experimental fission cross sections for $^{32}S + ^{138}Ba$ and $^{48}Ti + ^{122}Sn$. All energies are in the center-of-mass frame and are corrected to the center of the target. Errors include estimates of the systematic errors.

$^{32}S + ^{138}Ba$		$^{48}Ti + ^{122}Sn$	
Energy (MeV)	σ_{fiss} (mb)	Energy (MeV)	σ_{fiss} (mb)
133.3	72(10)	157.3	261(35)
129.2	38(6)	150.1	133(19)
125.3	15(3)	142.4	36(6)
121.4	5(3)	137.7	7(2)

The targets were produced by evaporating 170 $\mu g/cm^2$ and 175 $\mu g/cm^2$ of ^{138}BaO (isotopic purity 99.67%) and $^{122}SnO_2$ (isotopic purity 92.20%), respectively, onto 30 $\mu g/cm^2$ carbon foils [6]. Fission cross sections were measured for $^{32}S + ^{138}Ba$ and $^{48}Ti + ^{122}Sn$ for lab energies ranging from 150.0 to 164.7 MeV and 192.8 to 220.0 MeV, respectively. The energies (corrected for energy loss in the target) and cross sections are listed in Table I.

The fission fragments were detected in coincidence using Si surface barrier detectors. The forward detector was a $\Delta E - E$ telescope placed at approximately 55° in the center of mass for symmetric fission at each energy (32° − 38° in the laboratory). The solid angle subtended by the telescope detector was 2.60 msr. The thickness of the ΔE detector was 40 μm for the $^{32}S + ^{138}Ba$ and 30 μm for the $^{48}Ti + ^{122}Sn$ measurements. These thicknesses were chosen to provide good energy separation between the elastically scattered beam and the fission fragments while stopping only the fission fragments in the ΔE detector. The E detector was used to veto the elastically scattered beam particles.

The backward detector was a 100 μm Si strip detector. The detector consisted of seven independent strips. The dimension of each strip was 0.9 cm wide and 4 cm high. The strips were separated by 100 μm. Each strip was cross calibrated in energy using α particles and fission fragments from a ^{252}Cf fission source. The strip detector was centered at the complementary angle for a symmetric fission event in the forward detector (79° − 96° in the lab). Each strip of the detector subtended a horizontal angle of approximately 3.6°. The strip detector subtended a vertical angle of approximately 16.3° and was centered on the reaction plane defined by the beam and the telescope. The recoil scattering cross section in the strip detector was less than 10% of the Rutherford cross section in the forward telescope. However, most of the recoils were in the forward most strip of the detector, and some radiation damage to this strip was noted at the end of the experiment.

A 100 μmSi surface barrier detector was used as a beam monitor. This monitor was placed at 20° in the lab and subtended an angle of 0.3 msr.

III. DISCUSSION

The fission cross sections are determined from a subset of the events that were stopped in the forward ΔE detector and have a coincident fragment in any of the detector strips at backward angles.

The strip detector was centered at the complementary angle for each measurement. However, at the highest energies it was determined that some of the complementary fragments were beyond the forwardmost of the detector strips while the backwardmost detector strip had no fission events. The strip detector was moved forward in the angle to ensure that the detector was centered on the complementary fragment distribution. This resulted in the detector being centered $\sim 1.5°$ forward of the initial position, about half the solid angle of one strip, at the highest energy. At lower energies the displacement from the initial position was progressively less and was not necessary for the lowest energy measured. Figure 2 illustrates a typical complementary fragment distribution in the strip detector.

All events in the forward telescope were recorded to magnetic tape. The vetoing of the elastic particles was accomplished by removing all particles that produced a signal in the E detector of the telescope with a software gate. This process is approximately 90% effective for removing the elastic events and also allows the possibility of using the elastic cross section for normalization.

The fission events were identified in an $\Delta E - E_{strip}$ plot. Figure 3 shows a typical data plot where the results for all seven strip detectors are overlaid. In order to allow overlay of the various strips for comparison, the energy response of each of the various strip detectors was adjusted to provide a similar response to fission events from a ^{252}Cf source. The fission fragments are well separated in energy from the projectilelike and targetlike particles from inelastic scattering.

The placement of the fission detectors was chosen to minimize the angular distribution effects on the fission cross section. Thus the forward detector was placed at 55° in the center of mass for each measurement assuming that the compound nucleus decayed by symmetric fission. The fission cross sections derived from measurements at this angle are insensitive to assumptions on the shape

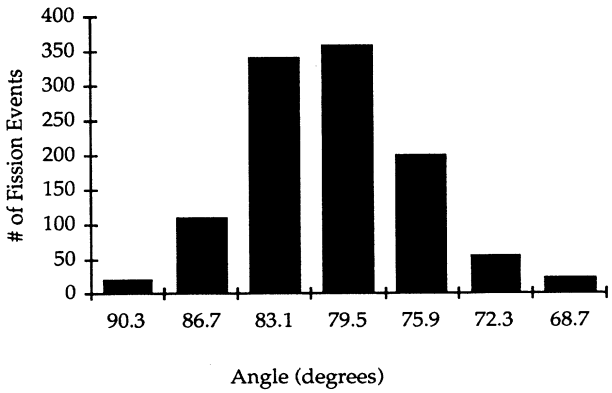

FIG. 2. Distribution of fission events in the strip detector for $^{48}Ti + ^{122}Sn$ at 220 MeV in the lab. Strip No. 1 is the backwardmost strip, and No. 7 is the forwardmost strip. Angles listed are in the laboratory frame and corresponds to the center of the strip. The position of the detector was chosen to be centered on this distribution for each measurement.

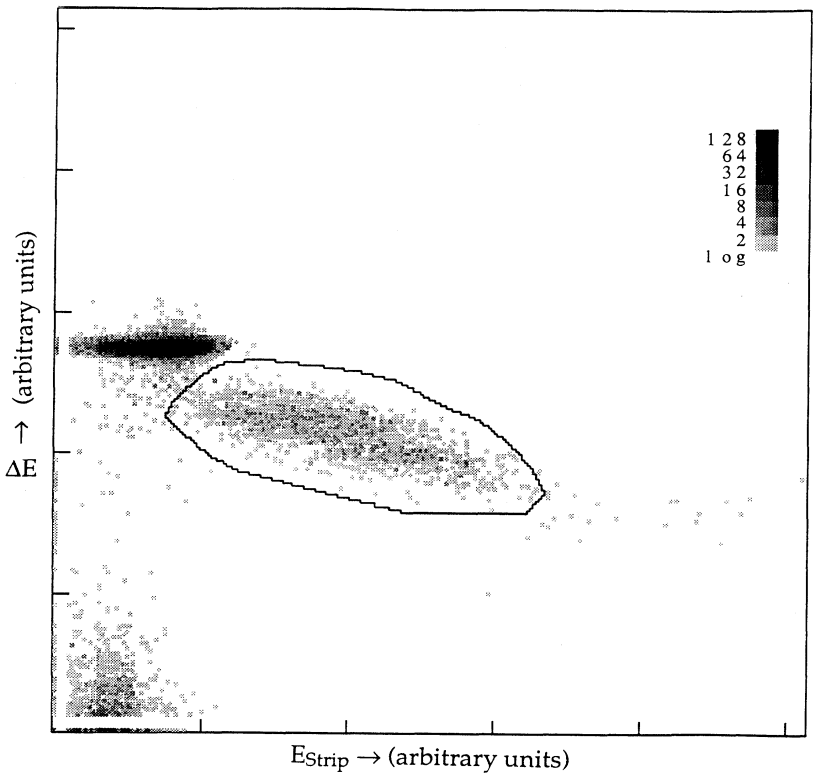

FIG. 3. ΔE vs E_{strip} for $^{48}\text{Ti}+^{122}\text{Sn}$ at 220 MeV in the lab. The spectra for each strip are overlaid to produce this plot. The energy response of each strip was calibrated using a ^{252}Cf source. The fission fragments are well separated from the elastic and inelastic events. The solid curve represents the gate used to identify the fission events. The axes are labeled in channel number.

of the angular distribution. It can be shown that the angle-integrated cross section is close to 4π times the differential cross section at this angle for distributions ranging from isotropic to those with an anisotropy larger than the expected anisotropy at the highest energy.

The fission cross section is determined relative to the elastic scattering cross section. Rutherford scattering is used for the elastic cross section and the fission cross section is given by

$$\sigma_{\text{Fiss}} = 4\pi \times \frac{N_{\text{Fiss}}}{2} \times \frac{1}{N_{\text{Elastic}}} \times \frac{d\sigma_{\text{Ruth}}}{d\Omega} \times \frac{J_{\text{Fiss}}}{J_{\text{Elastic}}} ,$$

where N_{Fiss} and N_{Elastic} are the area of the fission and the elastic peaks in the $\Delta E - E_{\text{Strip}}$ plot, respectively. The J_{Fiss} and J_{Elastic} terms are the Jacobians for the solid angle transformation from the lab frame to the center of mass frame for the fission and elastic channels, respectively. The thicknesses of the targets were also calculated from the area of the elastic peak at each energy and compared to the known thicknesses, providing an additional check on the analysis procedure. The fission cross sections are given in Table I for both systems and are shown as the shaded areas of the excitation functions shown in Fig. 4.

For the $^{28}\text{Si}+^{142}\text{Ce}$ system, the fission cross section was estimated using the statistical model PACE [7]. The input parameters for the PACE calculations were determined by fitting the evaporation residue yields measured by Gil *et al.* [2] for all three systems simultaneously. For the ^{32}S and ^{48}Ti systems, the fission cross sections measured here were also included in the determination of the parameters used in the statistical model.

The fission cross sections were combined with the evaporation residue cross sections of Gil *et al.* [2] to produce the total cross sections shown in Fig. 4. These excitation functions were fitted using the coupled channels code CCDEF [4]. The solid curves in Fig. 4 are from our coupled channels calculations. The dashed curves in Fig. 4 have some or all of the coupling terms in CCDEF turned off. With all the coupling turned off (uncoupled case in Fig. 4) represents the fusion cross sections from a simple one-dimensional barrier penetration model and illustrates the enhancement of the fusion cross section at sub-barrier energies. The parameters used in our coupled channels calculations are given in Table II along with the calculated barrier parameters.

In the coupled channels code CCDEF there are two possibilities for dealing with a quadrupole collective state. The first is to treat it as a collective surface vibration which is excited inelastically; this is the method commonly used for collective excitations in the coupled channels formalism [1]. The second possibility is to treat the quadrupole state as arising from a static deformation. In this case the barrier height and radius are calculated for each orientation and the fusion cross section is obtained by a weighted average over orientation. This procedure is similar to that proposed by Wong [8]. For our work here, we only used one or the other of these possibilities. This was to avoid the possibility of double counting the quadrupole contribution to the fusion cross section.

For the fits shown in Fig. 4, the deformation parameters for the first quadrupole and octupole states were taken from literature $B(E2)$ [9] and $B(E3)$ [10] values.

TABLE II. Parameters used in the CCDEF calculations for the solid curve in Fig. 4. For the quadrupole Q value (Q_2), an N/A indicates that the quadrupole channel was treated as a static deformation. The first three rows are the barrier parameters of the uncoupled curves in Fig. 4. Trans FF and Q_{Trans} are the coupling strength relative to a single particle transfer form factor and the Q value for the one neutron pickup channel, respectively.

System	^{28}Si + ^{142} Ce			^{32}S + ^{138} Ba			^{48}Ti + ^{122} Sn		
Property									
V_b		97.6			108.5			128.5	
R_b		11.23			11.09			11.56	
$\hbar\omega$		4.20			3.95			3.86	
β_2	0.41		0.12	0.31		0.09	0.27		0.10
Q_2	N/A		−0.64	N/A		−1.44	N/A		−1.14
β_3	0.40		0.13	0.48		0.13		0.19	0.12
Q_3	−6.88		−1.65	−5.01		−2.88	−3.36		−2.49
Trans FF		1.00			1.00			1.00	
Q_{Trans}		1.31			+0.03			−0.67	

The strength of the nuclear potential was then adjusted as a free parameter to get the best overall fit to the experimental data. In determining the quality of the fit the experimental points at above barrier energies were weighted more than points below the barrier. This fitting procedure leads to a small nonmonotonic dependence of the barrier radius.

A transfer channel was also included in the fits for all three systems using the Q values for one-neutron pickup. The Q values for neutron pickup are more positive than for neutron stripping. This improved the fits in the far sub-barrier region. The neutron stripping and proton stripping and pickup transfer channels discussed below have a minor effect and were not included in this fitting procedure.

One of the unresolved issues in sub-barrier fusion is the relative importance of collective excitations [11,12] and nucleon transfer [13,14] degrees of freedom. We can explore this issue with our CCDEF calculations which treat these degrees of freedom separately. In Fig. 4, two of the dashed curves show the relative contributions to the fusion cross section of the collective excitations only and of the one-particle transfer channels only. As mentioned above, the strengths of the collective excitations are known from the β values in the literature. The strengths of the transfer channels, however, are not known. We have used a default ($F = 1$) single particle strength for each transfer channel. In order to make a fair comparison between the couplings to collective excitations and to transfer channels, the same number of transfer channels were used for the transfer only calculations as for the collective only calculations. The total number of channels included for each was four. The collective states used are those discussed above. For the transfer couplings, in addition to the one neutron pickup transfer discussed above, couplings to the one neutron stripping, one proton pickup, and one proton stripping transfer channels were also included for the transfer-only calculations. The contribution of the transfer channel is minor in the ^{32}S + ^{138}Ba and ^{48}Ti + ^{122}Sn systems. For the ^{28}Si + ^{142} Ce system, transfer provides a significant contribution at energies below the barrier. These simple model calculations suggest that the primary contribution to the enhancement below the barrier is from the collective excitations. A definitive conclusion cannot be reached however without transfer cross section data and a coupled channels calculation which reproduces such data.

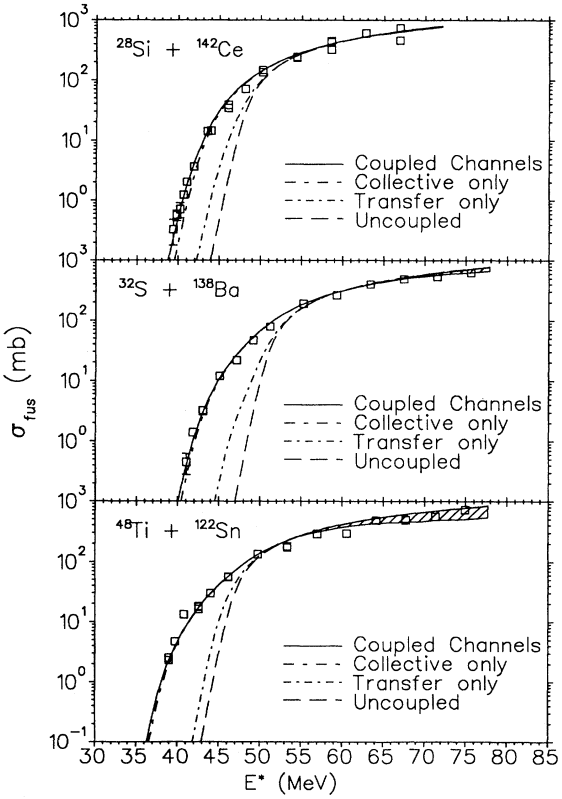

FIG. 4. Fusion excitation functions for ^{28}Si + ^{142} Ce, ^{32}S + ^{138} Ba, and ^{48}Ti + ^{122} Sn as a function of excitation energy in the compound nucleus. The shaded area represents the contribution of the experimentally measured fission cross section to the total fusion cross section. The solid curves are from coupled channels fits to the data as described in the text and using the parameters in Table II. The dashed curves are the same coupled channels calculations with some or all of the couplings turned off.

IV. CONCLUSION

We have measured the fusion-fission cross sections for two systems, $^{32}S + ^{138}Ba$, and $^{48}Ti + ^{122}Sn$, that produce the same compound nucleus, ^{170}Hf. These data was combined with the ER cross sections of Gil *et al.* [2] and analyzed using a simplified coupled channels calculation. We were able to reproduce the fusion cross sections for these systems using literature values for the deformation parameters. We would like to stress that for these calculations the only adjustable parameter was the depth of the nuclear potential. Our coupled channels calculations show that the primary contribution to the enhancement of the fusion cross section at energies below the Coulomb barrier for these systems comes from couplings to the collective states of the target and projectile nuclei and not from coupling to transfer channels.

The spin distributions from these coupled channels fits will be compared in a future report with experimental results from γ-ray multiplicity measurements in an effort to search for an entrance channel mass asymmetry effect on the fusion process at near-and sub-barrier energies [5].

This work was supported in part by the U.S. Department of Energy and the National Science Foundation.

[1] M. Beckerman, Phys. Rep. **129**, 145 (1985); S. Steadman and M. Rhoades-Brown, Ann. Rev. Nucl. Sci. **36**, 649 (1986); R. Vandenbosch, Ann. Rev. Nucl. Sci. **42**, 447 (1992).
[2] S. Gil *et al.* (unpublished)
[3] D. Digregorio, K. Lesko, B. Harmon, E. Norman, J. Pouliot, B. Sur, Y. Chan, and R. Stokstad, Phys. Rev. C **42**, 2108 (1990).
[4] J. Fernandez-Niello, C. Dasso, and S. Landowne, Comp. Phys. Comm. **54**, 409 (1989).
[5] A. Charlop, J. Bierman, Z. Drebi, A. Garcia, S. Gil, D. Prindle, A. Sonzogni, R. Vandenbosch, and D. Ye, the following paper, Phys. Rev. C **51**, 628 (1995).
[6] Micromatter, P. O. Box 123, Deer Harbor, Washington 98243-0123.
[7] A. Gavron *et al.*, Phys. Rev. Lett. **52**, 589 (1984).
[8] C. Y. Wong, Phys. Rev. Lett. **31**, 766 (1973).
[9] S. Raman, C. Malarkey, W. Milner, C. Nestor Jr., and P. Stelson, Nucl. Data Table **36**, 1 (1987).
[10] R. Spear, Nucl. Data Tables **42**, 55 (1989).
[11] H. Esbensen and S. Landowne, Phys. Rev. C **35**, 2090 (1987).
[12] H. Esbensen and S. Landowne, Nucl. Phys. **A492**, 473 (1989).
[13] P. H. Stelson, Phys. Lett. B **205**,190 (1988).
[14] P. H. Stelson, H. J. Kim, M. Beckerman, D. Shapira, and R. L. Robinson, Phys. Rev. C **41**, 1584 (1990).